Intercalibration of the split-window channels of SVISSR/FY-2C against AIRS/Aqua channels

JIANG Geng-ming[1], **YAN Hao**[2], **MA Ling-ling**[3]

1. *The Key Lab of Wave Scattering and Remote Sensing Information* (*MOE*), *Fudan University*, *Shanghai* 200433, *China*;
2. *National Meteorological Center*, *China Meteorological Administration*, *Beijing* 100081, *China*;
3. *Academy of Opto-electronics*, *Chinese Academy of Sciences*, *Beijing* 100190, *China*

Abstract: This paper addresses the intercalibration of the two split-window channels IR1 (10.9μm) and IR2 (11.9μm) of SVISSR (Stretched Visible and Infrared Spin Scan Radiometer) onboard the geostationary satellite FY-2C (FengYun 2C) against the most accurate and stable AIRS (Atmospheric Infrared Sounder) sensor onboard the polar-orbit satellite Aqua. The intercalibration was implemented using both the AIRS and SVISSR data around the equator in December of 2006 and 2007. The results reveal that: (1) the SVISSR data are highly linearly correlated with the convolved AIRS data, (2) calibration errors exist in SVISSR channels IR1 and IR2, and (3) the discrepancies become larger with time increment. With respect to the AIRS/Aqua measurements, when the brightness temperatures in SVISSR channels change from 220K to 340K, the temperature adjustment for IR1 in Dec., 2006 varies from 5.8K to −4.4K, and changes from 6.9K to −5.1K in Dec., 2007; The temperature adjustment for IR2 in Dec., 2006 goes from 2.2K to −1.5K, and varies from 6.3K to −6.1K in Dec., 2007.

Key words: intercalibration, SVISSR/FY-2C, AIRS/Aqua, split-window channels

CLC number: TP702/TP79 **Document code:** A

1 INTRODUCTION

The intercalibration is an operation that relates the outputs of a given instrument, in a certain spectral channel, to the output of one or more instruments measured in other channels (Asem *et al*., 1987; Butler & Barnes, 1998). Two methods, the Ray-Matching (RM) method (Doelling *et al*., 2004a, 2004b; Teillet *et al*., 2001; Heidinger *et al*., 2002) and the Radiative Transfer Modeling (RTM) method (Asem *et al*., 1987; Liu & Li, 2004; Vermote & Saleous, 2006) are commonly used in the intercalibration. Because of the spectral differences between conventional channels, both the RM and RTM methods have strengths and limitations: (1) The RM methods simply uses the conincident, co-angled and co-located measurements to transfer the calibration of one well-calibrated instrument to another, but it can not take into account the spectral differences between channels. The result may be unacceptable, if the spectral differences are large enough. (2) Although the RTM method can account for the spectral differences, the algorithm development is much more complicated, and it is also easily affected by the profile accuracy and the rediative transfer modeling.

FengYun 2C (FY-2C), the first geostationary meteorological satellite in China, was successfully launched at Xichang Satellite Launch Center, China, on October 19, 2004. FY-2C's main payload is the Stretched Visible and Infrared Spin Scan Radiometer (SVISSR). SVISSR/ FY-2C scans the Earth disc from north to south every 60 min with a nominal spatial resolution of 5 km in 5 spectral channels: the visible channel (0.73 μm), the water vapor channel (6.9 μm), the Mid-InfraRed (MIR) channel (3.8 μm) and the two split-window channels IR1 (InfraRed 1, 10.9 μm) and IR2 (InfraRed 2, 11.9 μm). The measurements in the two split-window channels of SVISSR/FY-2C are very suitable for the retrievals of the land/sea surface temperature, however the accurate calibration coefficients of the two split-window channels are not yet obtained, leading to uncertainties in the surface temperature retrieval.

As we know, the Atmospheric InfraRed Sounder (AIRS) onboard the polar-orbit satellite EOS Aqua is a hyper-spectral infrared sensor, containing 2378 infrared channels from 3.74μm to 15.39 μm and four visible/near-infrared channels ranging from 0.4 μm to 1.0 μm, and its spatial resolution is 13.5 km. The infrared radiance data product is stable to 10 mK/a and accurate to better than 250 mK, which is the most accurate and stable set of high spectral infrared measurements made in space to date (http://daac.gsfc.nasa.gov/AIRS/). Gunshor *et al*. (2007)

Received: 2008-05-16; **Accepted**: 2008-07-02

Foundation: Foundation of Fudan University for Young Scholars (08FQ06) and Research Foundation of National Microwave Sensing Laboratory.

First author biography: JIANG Geng-ming (1975—), male, assistant professor. He obtained the bachelor degree in photogrammetric engineering and remote sensing in 1997 from Wuhan Technical University of Surveying and Mapping, the master degree in geographical information system in 2003 from Institute of Remote Sensing Applications, Chinese Academy of Sciences, and the PhD degree in remote sensing in 2007 from Université Louis Pasteur-Strasbourg I. His research mainly focuses on quantitative remote sensing and digital image processing, and he has published more than 10 papers in this field. E-mail: jianggengming@hotmail.com

used the AIRS data to intercalibrate the water vapor channel and the split-window channels of the instruments onboard the geostationary satellites GOES (Geostationary Operational Environment Satellite), Meteosat-8 and MTSAT (Multi-functional Transport Satellite), and obtained good results. It should be noted that the spectral gaps over the AIRS water vapor spectral range will definitely affect the intercalibration accuracy, while the spectral gaps over the two split-window channels are very small, and can be negligible. As demonstrated in Fig. 1, the SVISSR channels IR1 and IR2 are fully covered by the AIRS hyper-spectral channels. Therefore, the use of the accurate hyper-spectral AIRS data to intercalibrate SVISSR/FY-2C infrared channels IR1 and IR2 not only has the advantages of both methods, but also avoid their limitations.

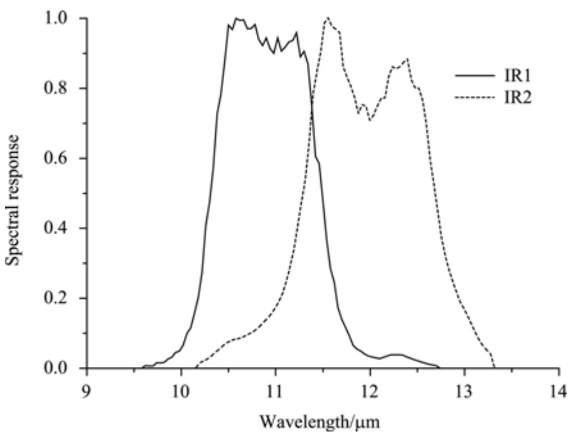

Fig. 1 Spectral responses of the channels IR1 (10.9μm) and IR2 (11.9μm) of SVISSR/FY-2C

In the following, this paper will be organized into four sections to address the intercalibration of the two split-window channels of SVISSR/FY-2C against AIRS/Aqua channels. Section 2 describes the intercalibration method; Section 3 presents the study area, data description and processing. Section 4 depicts the results and analysis, and the last section is devoted to the summary and conclusion.

2 METHOD

Based on the RM method, this work intercalibrated the two split-window channels of SVISSR/FY2C against AIRS/Aqua channels.

As mentioned previously, AIRS/Aqua possesses 2378 infrared channels varying from 3.74 μm to 15.39 μm, and the errors introduced by the small spectral gaps over the two split-window channels can be negligible. Assuming that the Spectral Response Functions (SRFs) of SVISSR/FY-2C channels IR1 and IR2 are accurate, the accurate measurement of SVISSR/FY-2C, R_i, can be predicted from the coincident, co-angled, co-located AIRS/Aqua measurements convolved with the SRFs of SVISSR channels IR1 and IR2, that is

$$R_i = \int_{\lambda_1}^{\lambda_2} f_i(\lambda) R_\lambda^{\text{AIRS}}(n) \mathrm{d}\lambda \Big/ \int_{\lambda_1}^{\lambda_2} f_i(\lambda) \mathrm{d}\lambda \quad (1)$$

where $f_i(\lambda)$ is the SRF of SVISSR channel i, λ_1 and λ_2 are the lower and upper limits, respectively, $R_\lambda^{\text{AIRS}}(n)$ is the measurement in AIRS channel n at wavelength λ.

In the coincident, co-anlged, co-located conditions, the actual SVISSR/FY-2C measurements were regressed against the AIRS/Aqua measurements calculated using Eq. (1), and then the intercalibration coefficients of the two split-window channels of SVISSR/FY-2C were obtained.

3 STUDY AREA, DATA DESCRIPTION AND PROCESSING

As we know, FY-2C locates above the equator with an altitude of 36,000 km and longitude of 105°E, and the SVISSR/FY-2C instrument scans the Earth disc from north to south every 60 min to acquire a normalized disc images centered at (105°E, 0). While the AIRS instrument is onboard the polar-orbit satellite EOS Aqua, and scans the Earth surface across the track. During daytime, EOS Aqua ascends across the equator, while it descends the equator at night. According to the view geometries of both SVISSR/FY-2C and AIRS/Aqua, the coincident, co-angled, co-located measurements are only distributed in the small area centered at (105°E, 0) and perpendicular to the EOS Aqua's track. Therefore, the following qualified study area was selected: the longitude goes from 59.5°E to 149.5°E and the latitude changes from 10.0°S to 10.0°N (Fig. 2), and was divided into small pixels with sizes of 0.5°×0.5° in term of the spatial resolutions of both SVISSR/FY-2C and AIRS/Aqua data. As shown in Fig. 2, the selected study area is mainly water, and small portions of vegetated land surface are also included.

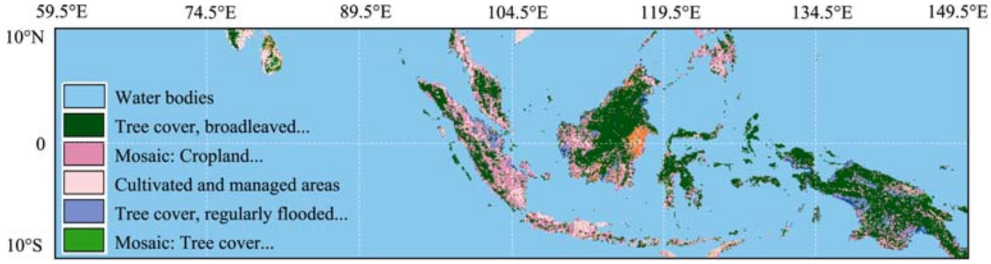

Fig. 2 Study area generated from the Global Land Cover 2000

The geolocated and calibrated SVISSR/FY-2C Normalized dataset and the AIRS/Aqua L1B data product covering the study area in Dec. of 2006 and Dec. of 2007 (Total 60 days) were used in this work. The brightness temperatures at top of atmosphere (TOA) in SVISSR channels IR1 and IR2, the view zenith angle, the sun zenith angle and the relative azimuth angle were extracted from the SVISSR/FY-2C Normalized dataset. In contrast to the data extraction from the SVISSR/FY-2C Normalized dataset, the processing of the AIRS/Aqua L1B data is more complicated. The radiances in the channels fallen into the SVISSR channels IR1 and IR2, longitude, latitude, view zenith angle, view azimuth angle, sun zenith angle and sun azimuth angle were firstly extracted from the AIRS/Aqua L1B data product, and then the integrated AIRS/Aqua measurements over SVISSR channels IR1 and IR2 were calculated using Eq. (1). Finally, the integrated radiances were converted into brightness temperatures using look-up tables. It should be mentioned that the nighttime AIRS/Aqua L1B data product does not contain the sun azimuth angle, and the night sun azimuth angle was calculated pixel by pixel in term of the coordinates and time.

In order to spatially match SVISSR/FY-2C measurements with the integrated AIRS/Aqua measurements, all data were aggregated into the study area with pixel sizes of 0.5°× 0.5° base on the following pixel aggregation formula

$$R(i)=\sum_{j=1}^{N}\omega(j)R(j)/\sum_{j=1}^{N}\omega(j) \quad \text{with } \omega(j)=S_{\mathrm{p}}(j)/S(j) \tag{2}$$

where $R(i)$ is the pixel aggregated radiance (output), N is the total number of pixels involved in the aggregation, $\omega(j)$ is the weighting factor of input pixel j, $S_{\mathrm{p}}(j)$ is the overlapping area between the input pixel j and output pixel i, $S(j)$ is the total area of input pixel j, and $R(j)$ is the radiance of input pixel j.

In practice, the coincident, co-angled, co-located measurements are rare, and the approximate conditions are usually used. The coincident or approximate coincident condition can be substituted by the equal or approximate equal sun angles. Considering the practical situations, this work adopted the following matching conditions: the absolute view zenith angle difference (|ΔVZA|) less than 2.0°, the absolute sun zenith angle difference ((|ΔSZA|) less than 2.0°, and the absolute relative azimuth angle difference ((|ΔRAA|) less than 5.0°. There are 90 SVISSR/FY-2C images and 240 AIRS/Aqua images qualified the approximate matching conditions in Dec. of 2006 and Dec. of 2007, respectively, and observation time ranges from 3:00UTC to 9:00UTC and from 15:00UTC to 21:00UTC.

Another problem is that accurate coordinate matching should be performed between the pixel aggregated SVISSR/FY-2C images and the AIRS/Aqua images. If two images are accurately matched, the Root Mean Square Error (RMSE) of the differences between the two images is minimum, which is called the minimum RMSE principle here. Based on the minimum RMSE principle, the accurate coordinate matching between the aggregated SVISSR/FY-2C images and the aggregated AIRS/Aqua images was realized in the following steps: the coordinate matching pixels were firstly picked out from the aggregated images, and then the accurate coordinate matching was carried out between the images in which coordinate matching pixels exist, and finally the accurate coordinate matching pixels were searched out from the accurately coordinate matched images.

4 RESULTS AND ANALYSIS

There are about 1,000 qualified measurement pairs with absolute view zenith angle difference less than 2.0°, absolute sun zenith angle difference less than 2.0° and absolute relative azimuth angle difference less than 5.0° in Dec. of 2006 and Dec. of 2007, respectively. In this work, the actual SVISSR/FY-2C measurements were taken as X-axis, while the integrated AIRS/Aqua measurements were taken as Y-axis, and then the linear regression were performed between them (Fig. 3). Fig. 3(a) and 3(b) show that the SVISSR measurements are highly correlated to the integrated AIRS measurements in the temperature range from 180.0 K to 300.0 K, and the correlation coefficients are greater than 0.97. In relation to the AIRS instrument, there are large calibration errors existing in the two split-window channels of SVISSR/FY-2C, in which the calibration coefficients for SVISSR IR2 channel are largely changed from Dec. of 2006 to Dec. of 2007 and have a tendency to become larger, while the calibration coefficients for SVISSR IR1 channel have relatively small discrepancies. In order to further analyze the results, the difference between the integrated AIRS measurement and the SVISSR measurement is defined as the temperature adjustments in the SVISSR channel, and its variation with the brightness temperature was examined. When the brightness temperatures in SVISSR channels vary from 220K to 340K, the temperature adjustment in SVISSR IR1 channel changes linearly from 5.8K to −4.4K in Dec. of 2006, and from 6.9K to −5.1K in Dec. of 2007; The temperature adjustment in SVISSR IR2 channel linearly goes from 2.2K to −1.5K in Dec. of 2006, and from 6.3K to 6.3K to −6.1 K. in Dec. of 2007 (Fig. 3(c)).

It should be noted that, the distribution of the measurement pairs is scattered and the RMSEs are greater than 4.0 K as shown in Fig. 3(a) and 3(b). This may due to the use of the approximate matching constraints, e.g., not only the surface temperature changes with time, but also the atmospheric water vapor content and the cloud contamination, which leads to differences between the matching measurements. However, the results are not strongly affected by this because the differences counteract each other in the linear regression based on large amount of measurements.

Based on the results presented above, the following Eqs. (3) and (4) are used to re-calibrate the two split-window channels in Dec. of 2006 and Dec. of 2007, respectively, in relation to the AIRS/Aqua instrument:

$$\text{Dec., 2006:} \quad \begin{cases} T_{\mathrm{b,IR1,R}} = 24.54 + 0.915T_{\mathrm{b,IR1}} \\ T_{\mathrm{b,IR2,R}} = 9.04 + 0.969T_{\mathrm{b,IR2}} \end{cases} \tag{3}$$

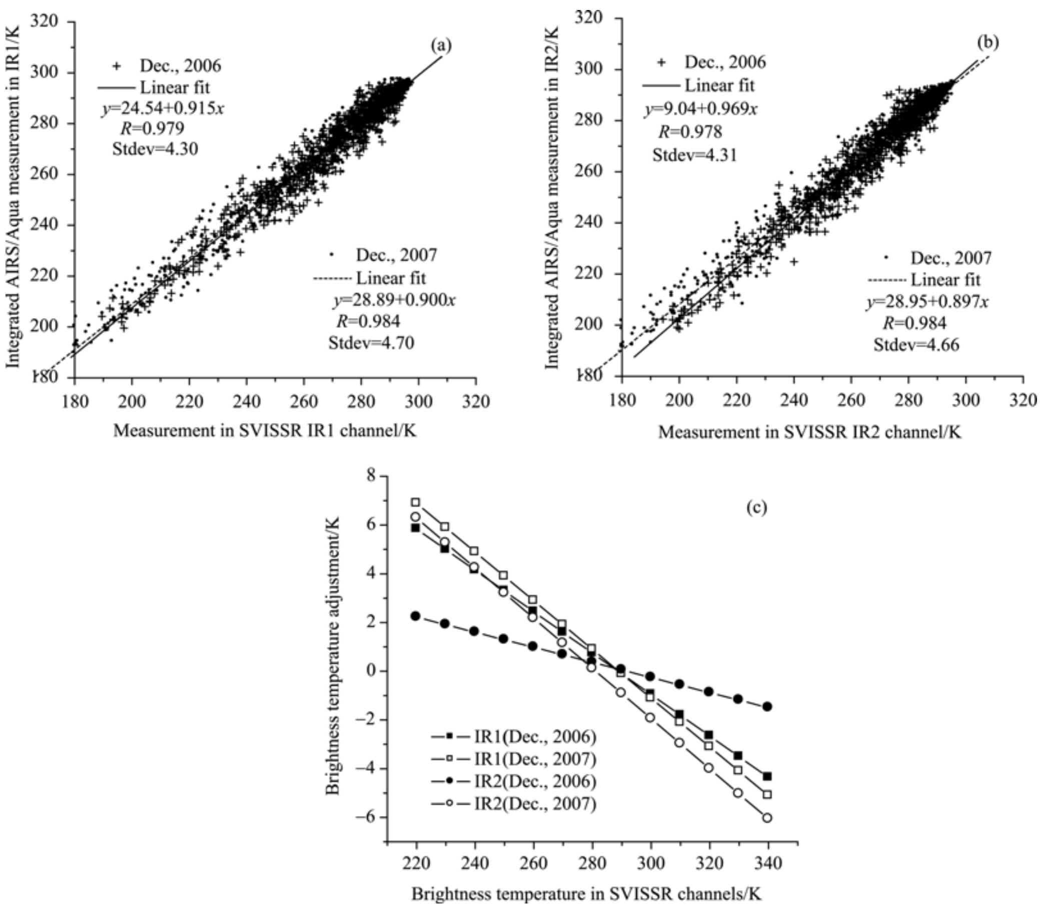

Fig. 3 Ray-matching observations between the convolved AIRS measurements and SVISSR measurements and results of the linear statistical analysis

(a) For IR1; (b) For IR2; (c) Brightness temperature adjustments for SVISSR/FY-2C channels IR1 and IR2 with respect to the AIRS/Aqua measurements (*R* represents correlation coefficient; Stdev denotes standard deviation)

$$\text{Dec., 2007:}\quad \begin{cases} T_{\mathrm{b,IR1,R}} = 28.89 + 0.900 T_{\mathrm{b,IR1}} \\ T_{\mathrm{b,IR2,R}} = 28.95 + 0.897 T_{\mathrm{b,IR2}} \end{cases} \tag{4}$$

in which, $T_{\mathrm{b,\ IR1}}$ and $T_{\mathrm{b,IR2}}$ are, respectively, actually measured brightness temperatures in SVISSR channels IR1 and IR2, while $T_{\mathrm{b,IR1,R}}$ and $T_{\mathrm{b,IR2,R}}$ are, respectively, the intercalibrated brightness temperatures in SVISSR channels IR1 and IR2.

5 SUMMARY AND CONCLUSION

This paper addressed the intercalibration of the split-window channels of SVISSR/FY-2C with the AIRS/Aqua channels. According to the characteristics of the observing geometries of the AIRS/Aqua and SVISSR/FY-2C instruments, the study area with longitude varying from 59.5°E to 149.5°E and latitude going from 10.0°S to 10.0°N, and Dec. of 2006 and Dec. of 2007 were selected in this work. The integrated measurements over SVISSR channels IR1 and IR2 were firstly calculated using Eq. (1), and then both the integrated AIRS/Aqua measurements and the SVISSR/FY-2C measurements were pixel aggregated into the study area using Eq. (2). The intercalibration was implemented using both the co-located AIRS and SVISSR data with |ΔVZA|<2.0°, |ΔSZA |<2.0° and |ΔRAA|< 5.0°.

The results indicate that calibration errors exist in SVISSR channels IR1 and IR2, and become larger with time. When the brightness temperature in the SVISSR channel changes from 220 K to 340 K, the brightness temperature adjustment in IR1 linearly goes from 5.8 K to −4.4 K in Dec. of 2006, and from 6.9 K to −5.1 K in Dec. of 2007, while it linearly varies from 2.2 K to −1.5 K in IR2 in Dec. of 2006, and from 6.3 K to −6.1 K in Dec. of 2007.

In this work, the intercalibration was carried out only in two months, and intercalibration coefficients and their variation with time in long term should be obtained to fully understand the operational conditions of the SVISSR/FY-2C instrument. The intercalibration method described in this paper can be also applied to other FengYun series of satellites.

REFERENCES

Asem A, Deschamps P Y and Ho D. 1987. Calibration of METEOSAT infrared radiometer using split-window channels of NOAA AVHRR. *Journal of Atmospheric and Oceanic Technology*, **4**(4): 553−562

Butler J and Barnes R A. 1998. Calibration strategy for the Earth Observing System (EOS)-AM1 platform. *IEEE Transactions on Geoscience and Remote Sensing*, **36**(4): 1056—1061

Doelling D R, Nguyen L and Minnis P. 2004a. Calibration comparisons between SEVIRI, MODIS, and GOES data. Proc. 2004 EUMETSAT Meteorological Satellite Conference, Prague, Czech Republic

Doelling D R, Minnis P and Nguyen L. 2004b. Calibration comparisons between SEVIRI, MODIS, and GOES data. MSG RAO workshop. Salzburg, Austria

Gunshor M M, Schmit T J, Menzel W P and Tobin D. 2007. Intercalibration of the newest geostationary imagers via high spectral resolution AIRS data. Atmospheric and Environmental Remote Sensing Data Processing and Utilization III: Readiness for GEOSS, San Diego, CA. Proc. SPIE Int. Soc. Opt. Eng. 6684, 66841H

Heidinger A K, Cao C and Sullivan J T. 2002. Using moderate resolution imaging spectrometer (MODIS) to calibrate advanced very high resolution radiometer reflectance channels. *Journal of Geophysical Research*, 107 (D23): 4702

Liu J J and Li Z. 2004. A new method for cross-calibration of two satellite sensors. *International Journal of Remote Sensing*, **25**(23): 5267—5281

McMillin L M. 1975. Estimation of sea surface temperature from two infrared window measurements with different absorption. *Journal of Geographical Research*, **80**: 5113—5117

Sobrino J A and Romaguera M. 2004. Land surfacemperature retrieval from MSG1-SEVIRI data. *Remote Sensing of Environment*, **92**: 247—254

Teillet P M, Barker J L, Markham B L, Irish R R, Fedosejevs G and Storey J C. 2001. Radiometric cross-calibration of the Landsat-7 ETM+ and Landsat-5 TM sensors based on tandem data sets. *Remote Sensing of Environment*, **78**: 39—54

Vermote E F and Saleous N Z. 2006. Calibration of NOAA16 AVHRR over a dersert site using MODIS data. *Remote Sensing of Environment*, **105**: 214—220

Wan Z and Dozier J. 1996. A generalized split-window algorithm for retrieving land-surface temperature from space. *IEEE Transections on Geoscience and Remote Sensing*, **34**(4): 892—905

利用 AIRS 数据交叉辐射定标 SVISSR 分裂窗通道

蒋耿明[1], 延 昊[2], 马灵玲[3]

1. 复旦大学 波散射与遥感信息教育部重点实验室, 上海 200433;
2. 中国气象局 国家气象中心, 北京 100081;
3. 中国科学院 光电研究院, 北京 100190

摘 要: 利用高精度和稳定的 AIRS/Aqua(Atmospheric InfraRed Sounder on board Aqua)数据对 SVISSR/FY-2C(Stretched Visible and Infrared Spin Scan Radiometer onboard FengYun 2C)的两个分裂窗通道 IR1(InfraRed 1, 10.9 μm)和 IR2(InfraRed 2, 11.9μm)进行交叉辐射定标的方法, 并利用赤道附近 2006 年 12 月和 2007 年 12 月的 AIRS 和 SVISSR 数据完成了交叉辐射定标, 结果表明, SVISSR 数据与卷积得到的 AIRS 数据高度线性相关, SVISSR/FY-2C 传感器的两个分裂窗通道不仅存在定标误差, 而且定标误差随时间的变化呈现增大的趋势。相对于 AIRS/Aqua 测量值, 当 SVISSR 的通道亮温从 220 K 变化到 340 K 时, 2006 年 12 月 IR1 通道的温度调整量从 5.8 K 变化到−4.4 K, 而 2007 年 12 月 IR1 通道的温度调整量从 6.9 K 变化到−5.1 K; 2006 年 12 月 IR2 通道的温度调整量从 2.2 K 变化到−1.5 K, 而 2007 年 12 月 IR2 通道的温度调整量从 6.3 K 变化到−6.1 K。

关键词: 交叉辐射定标, SVISSR/FY-2C, AIRS/Aqua, 分裂窗通道

中图分类号: TP702/TP79 **文献标识码:** A

1 引 言

交叉辐射定标是建立一个传感器特定通道的输出与另一个或多个传感器在其他通道的输出之间的关系, 并把经过精确定标的传感器的定标参数传给其他传感器(Asem 等, 1987; Butler 等, 1998)。常用的交叉辐射定标方法有光线匹配(Ray-Matching, RM)方法(Doelling 等, 2004a, 2004b; Teillet 等, 2001; Heidinger 等, 2002)和辐射传输模拟(Radiative Transfer Modeling, RTM)方法(Asem 等, 1987; Liu & Li, 2004; Vermote & Saleous, 2006)。由于以前卫星传感器通道之间的差异, 这两种方法各有优缺点: (1) RM 方法直接通过对不同传感器获取到的同时间、同地点和同角度的观测进行比对来实现交叉辐射定标, 简单明了, 但是该方法不能顾及到通道之间的光谱差异。如果通道之间的光谱差异过大, 可能导致不可接受的误差。(2) 虽然 RTM 方法可以消除光谱差异引起的交叉定标误差, 但算法过于复杂, 而且也容易受大气廓线测量精度和辐射传输计算或模拟的影响。

2004-10-19, 中国在西昌卫星发射中心成功地发射了一颗静止气象卫星——“风云二号”C 星(FY-2C), 定位于 105ºE 的赤道上空。FY-2C 搭载的主要仪器设备是可伸展的可见光和红外自旋转扫描辐射计(Stretched Visible and Infrared Spin Scan Radiometer, SVISSR)。SVISSR 探测器的星下点空间分辨率是 5km, 每隔 60min 从北向南扫描获取一幅圆盘影像。SVISSR 探测器共有 5 个通道: 一个可见光通道(0.73μm)、一个水汽通道(6.9μm)、一个中红外通道(3.8μm)和两个分裂窗通道 IR1(InfraRed 1, 10.9μm)和 IR2(InfraRed 2, 11.9μm), 其中, 两个分裂窗通道的设置非常适合从卫星观测值反演地表和海表温度(McMillin, 1975; Wan & Dozier, 1996; Sobrino & Romaguera, 2004), 但是这两个通道的在轨定标参数还没有精确测定, 直接影响到温度反演的精度。

收稿日期: 2008-05-16; 修订日期: 2008-07-02

基金项目: 复旦大学青年科学基金(08FQ06)和国家 863 计划微波遥感技术实验室研究基金。

第一作者简介: 蒋耿明(1975—), 男, 博士, 本科于 1997 年 6 月毕业于武汉测绘科技大学摄影测量与遥感专业, 硕士, 于 2003 年 6 月毕业于中国科学院遥感应用研究所制图学与地理信息系统专业, 博士于 2007 年 10 月毕业于法国斯特拉斯堡第一大学遥感专业, 现为复旦大学信息科学与工程学院讲师。主要研究领域为定量遥感和数字图像处理。

大气红外探空器(Atmospheric InfraRed Sounder, AIRS)搭载在地球极轨卫星 Aqua 上，是一种高光谱红外空间探测器，拥有 2378 个红外通道，覆盖 3.74—15.39μm 的波谱范围，拥有 4 个波长 0.4—1.0μm 的可见光和近红外通道，其星下点的空间分辨率是 13.5 km。AIRS 红外数据产品非常稳定，偏移量低于 10 mK/a，测温精度优于 250 mK，大多数通道的绝对定标精度达到 100 mK，是目前最精确和最稳定的高光谱红外辐射光谱测量数据(http://daac.gsfc.nasa.gov/AIRS/)。Gunshor 等(2007)利用 AIRS 数据对 GOES、Meteosat-8 和 MTSAT 系列静止卫星的水汽通道和分裂窗通道进行了交叉辐射定标，取得了很好的效果，但是 AIRS 在水汽通道的光谱间隙对定标存在较大的影响，在两个分裂窗通道的光谱间隙很小，可以忽略不计。AIRS 传感器的光谱范围完全覆盖 SVISSR 的两个分裂窗通道 IR1 和 IR2(图 1)，利用高精度和高光谱 AIRS 数据对 SVISSR 传感器的两个分裂窗通道进行精确定标，不仅拥有 RM 和 RTM 方法的优点，而且避免了其缺点。

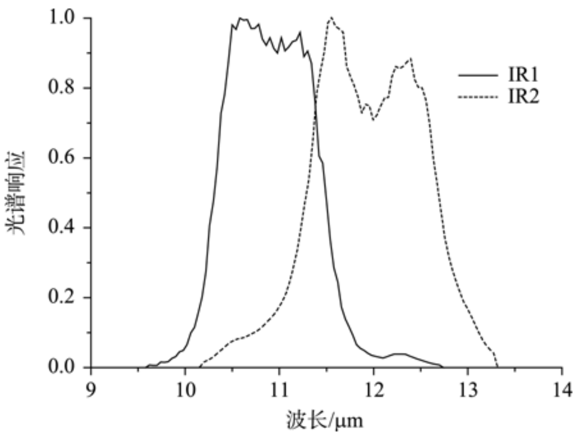

图 1 SVISSR 传感器两个分裂窗通道 IR1(10.9μm)和 IR2(11.9μm)的波谱响应函数

2 基本方法

研究基于 RM 方法，以 AIRS/Aqua 传感器为标准对 SVISSR/FY-2C 传感器的两个分裂窗通道进行交叉辐射定标。

假设 SVISSR 的光谱响应函数(Spectral Response Function, SRF)是精确的，将 AIRS/Aqua 数据分别与 SVISSR 的两个分裂窗通道的光谱响应函数进行卷积计算，得到与 AIRS 传感器同地点、同角度和同时间的 SVISSR 传感器的精确观测值 R_i，即：

$$R_i = \int_{\lambda_1}^{\lambda_2} f_i(\lambda) R_\lambda^{\text{AIRS}}(n) \mathrm{d}\lambda \Big/ \int_{\lambda_1}^{\lambda_2} f_i(\lambda) \mathrm{d}\lambda \tag{1}$$

式中，$f_i(\lambda)$是 SVISSR 传感器第 i 通道的光谱响应函数，λ_1 和 λ_2 是光谱响应函数的下限和上限，$R_\lambda^{\text{AIRS}(n)}$ 是 AIRS/Aqua 传感器波长为 λ 的第 n 通道的观测值。

在同地点、同时间和同角度的观测条件下，SVISSR 传感器的实际观测值与利用上述公式(1)进行卷积计算得到的辐射值进行比对和回归分析，得到 SVISSR 传感器通道的交叉辐射定标系数。

3 研究区域、数据描述和处理

如前文所述，SVISSR/FY-2C 传感器定位于 105°E 的赤道上空，从北向南扫描地球表面，获取的标称影像是以(104.5°E, 0)为中心的一个圆盘。AIRS 传感器搭载在极轨卫星 Aqua 上，垂直于卫星轨迹方向扫描地球表面；白天，Aqua 卫星从南向北斜穿赤道，晚上从北向南斜穿赤道。根据 SVISSR/FY-2C 和 AIRS/Aqua 传感器对地观测的几何特点，地点、时间和角度相同或相近的观测只能位于以(104.5°E, 0)为中心，垂直于 Aqua 卫星运动轨迹方向的狭窄区域里。因此，满足条件的区域是：纬度从 10.0ºS—10.0°N，经度 59.5°E—149.5°E(图 2)，根据 SVISSR 和 AIRS 数据的空间分辨率把该研究区域划分成 0.5°×0.5°的像素单元。如图 2，研究区域绝大部分是水体，还有一些被植被覆盖的陆地。

利用 2006 年 12 月和 2007 年 12 月(共 60 天)覆盖研究区域经过空间定位和辐射定标的 SVISSR/FY- 2C 标称数据和 AIRS/Aqua L1B 数据。利用自主开 发的程序从 SVISSR 数据文件中提取 IR1 和 IR2 通道大气顶的亮温数据以及卫星天顶角、太阳天顶角和相对方位角数据。

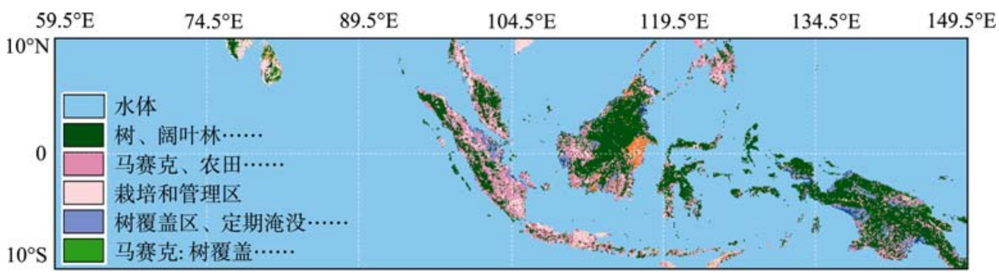

图 2 研究区域(根据 Global Land Cover 2000 数据绘制)

相对 SVISSR 数据的提取，AIRS 数据处理要复杂一些：首先，从 AIRS 数据文件中提取覆盖 SVISSR IR1 和 IR2 波谱范围的所有通道数据以及经度数据、纬度数据、卫星天顶角、卫星方位角、太阳天顶角和太阳方位角；然后，分别对 AIRS 辐射值数据与 SVISSR IR1 和 IR2 两个通道的光谱响应函数进行卷积计算，得到 AIRS 在 IR1 和 IR2 通道上的观测值；最后，利用辐射值-温度转换查找表，把卷积得到的辐射值转换成亮温。另外，夜晚的 AIRS 数据的太阳方位角为空白，根据 AIRS 数据的经纬度坐标和观测时间，计算得到 AIRS 数据晚上的太阳方位角。

为了对 SVISSR 影像和卷积得到的 AIRS 影像进行空间匹配，需要把所有的数据聚合到上述 0.5°×0.5°的研究区域，这里采用如下基于面积加权的像素聚合公式来实现：

$$R(i)=\sum_{j=1}^{N}\omega(j)R(j)/\sum_{j=1}^{N}\omega(j) \quad (2)$$

式中，$\omega(j)=S_{\mathrm{p}}(j)/S(j)$，$R(i)$是经过像素聚合得到的第 i 点的辐射值，即输出像素辐射值，N 是输入像素总数，$\omega(j)$是输入像素 j 的权重因子，$S_{\mathrm{p}}(j)$是输入像素 j 与输出像素 i 的重叠部分面积，$S(j)$是输入像素 j 的总面积，$R(j)$是输入像素 j 的辐射值。

在现实中，很难找到角度和时间完全相同的观测，一般采用角度和时间近似相等的匹配条件。时间相等或近似相等的条件可以用太阳角度相等或近似相等的条件替代。根据实际情况，本研究采用下述匹配条件：观测天顶角之差的绝对值(|ΔVZA|)<2.0°，太阳天顶角之差的绝对值(|ΔSZA|)<2.0°和相对方位角之差的绝对值(|ΔRAA|)<5.0°。2006 年 12 月和 2007 年 12 月各有~90 幅 FY-2C 数据和~240 幅 AIRS/Aqua 数据满足上述近似匹配条件，且卫星数据分布在格林威治时间(UTC)3:00—9:00 和 15:00—21:00 两个时间段内。

SVISSR 影像和卷积得到的 AIRS 影像经过像素聚合后在坐标上需精确配准。考虑到如果两幅影像是精确配准的，它们之间的均方根差(Root Mean Square Error, RMSE)一定是最小的，这里称之为均方根差最小原则。这样，根据均方根差最小原则，可以采用如下方法实现两幅影像的坐标精确配准：(1)搜索到满足上述近似匹配条件的点；(2)对存在匹配点对的影像根据最小均方根差原则对两幅聚合后的影像进行精确坐标配准。在坐标精确配准后的影像里，再次逐像素搜索出满足上述近似匹配条件的所有观测点对。

4 结果和分析

满足同地点、|ΔVZA|<2.0°、|ΔSZA|<2.0°和|ΔRAA|<5.0°的 SVISSR 和 AIRS 观测点对在 2006 年 12 月和 2007 年 12 月分别有大约 1000 对观测值。SVISSR 的实际观测值作 X 轴变量，卷积得到的 AIRS 观测作 Y 轴变量，分别对两个月的观测点对进行线性回归分析，并把结果绘制在图 3 中。图 3(a)和

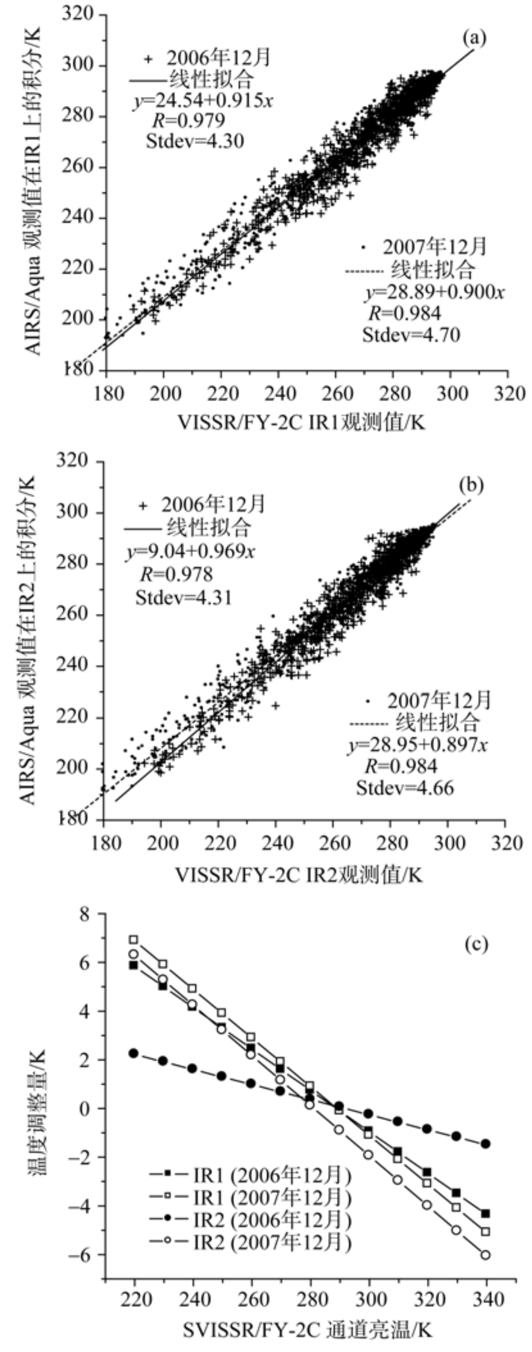

图 3 卷积得到的 AIRS 观测值与 SVISSR 观测值之间的关系以及线性统计分析

(a) IR1 通道; (b) IR2 通道; (c) 相对于 AIRS/Aqua 测量值的 SVISSR/FY-2C 通道 IR1 和 IR2 的温度调整量(R 代表相关系数; Stdev 代表标准方差)

(b)显示 SVISSR 观测值和卷积得到的 AIRS 观测值在 180—300K 的温度范围内具有很高的线性相关性，相关系数大于 0.97。相对于 AIRS 传感器，SVISSR 传感器的两个分裂窗通道存在较大的定标误差，其中 2006 年 12 月和 2007 年 12 月的 SVISSR IR1 通道的辐射定标变化不是很大，而 SVISSR IR2 通道的辐射定标系数在这两个月内发生了较大的变化，且随时间的变化而呈现增大的趋势。为了进一步对结果进行分析，把卷积得到的 AIRS 与 SVISSR 观测值之间的差定义为 SVISSR 传感器通道的亮温调整量，统计其随亮温变化的情况。当 SVISSR 的通道亮温从 220K 变化到 340K 时, 2006 年 12 月 IR1 通道的亮温调整量从 5.8K 线性变化到–4.4K，而 2007 年 12 月 IR1 通道的亮温调整量从 6.9K 线性变化到–5.1K; 2006 年 12 月 IR2 通道的亮温调整量从 2.2K 线性变化到–1.5K，而 2007 年 12 月 IR2 通道的亮温调整量从 6.3K 线性变化到–6.1K(图 3(c))。

另外，图 3(a)、(b)中的匹配点对比较离散，线性回归的标准方差均大于 4.0K，这是因为该研究采用角度和时间近似相等的匹配条件，例如：时间不同，不仅下垫面的温度发生了变化，而且大气水汽含量和云覆盖也会发生变化，导致匹配点对的温差异常。但是，这种离散对基于大量点对的线性回归分析是相互抵消的，因此对最终结果不会造成大的影响。

综上所述，相对于 AIRS/Aqua 传感器, SVISSR/FY-2C 传感器的两个分裂窗通道在 2006 年 12 月和 2007 年 12 月的辐射定标分别采用下面的公式(3)和公式(4):

2006 年 12 月:

$$\begin{cases} T_{\mathrm{b,IR1,R}} = 24.54 + 0.915 T_{\mathrm{b,IR1}} \\ T_{\mathrm{b,IR2,R}} = 9.04 + 0.969 T_{\mathrm{b,IR2}} \end{cases} \tag{3}$$

2007 年 12 月:

$$\begin{cases} T_{\mathrm{b,IR1,R}} = 28.89 + 0.900 T_{\mathrm{b,IR1}} \\ T_{\mathrm{b,IR2,R}} = 28.95 + 0.897 T_{\mathrm{b,IR2}} \end{cases} \tag{4}$$

式中，$T_{\mathrm{b,IR1}}$ 和 $T_{\mathrm{b,IR2}}$ 分别是 SVISSR IR1 和 IR2 两个通道的实际观测亮温，而 $T_{\mathrm{b,IR1,R}}$ 和 $T_{\mathrm{b,IR2,R}}$ 分别是交叉辐射定标后 SVISSR IR1 和 IR2 两个通道的亮温。

5 结 论

本文利用高精度和稳定的 AIRS/Aqua 数据对 SVISSR/FY-2C 的两个分裂窗通道进行交叉辐射定标。

实验结果表明, SVISSR 传感器的 IR1 和 IR2 通道存在辐射定标误差，且随着时间的变化而呈现增大的趋势。当 SVISSR 的通道亮温从 220 K 变化到 340 K 时，2006 年 12 月 IR1 通道的亮温调整量从 5.8K 线性变化到–4.4K，而 2007 年 12 月 IR1 通道的亮温调整量从 6.9K 线性变化到–5.1K; 2006 年 12 月 IR2 通道的亮温调整量从 2.2K 线性变化到–1.5K，而 2007 年 12 月 IR2 通道的亮温调整量从 6.3K 线性变化到–6.1 K。

本文只进行了两个月的交叉辐射定标，要全面掌握 SVISSR/FY-2C 传感器的辐射定标情况，还需要进一步测定 SVISSR/FY-2C 传感器 IR1 和 IR2 通道的定标系数，以及其随时间的变化规律。该方法也可以应用到其他“风云”系列卫星的辐射定标。

REFERENCES

Asem A, Deschamps P Y and Ho D. 1987. Calibration of METEOSAT infrared radiometer using split-window channels of NOAA AVHRR. *Journal of Atmospheric and Oceanic Technology*, **4**(4): 553—562

Butler J and Barnes R A. 1998. Calibration strategy for the Earth Observing System (EOS)-AM1 platform. *IEEE Transactions on Geoscience and Remote Sensing*, **36**(4): 1056—1061

Doelling D R, Nguyen L and Minnis P. 2004a. Calibration comparisons between SEVIRI, MODIS, and GOES data. Proc. 2004 EUMETSAT Meteorological Satellite Conference, Prague, Czech Republic

Doelling D R, Minnis P and Nguyen L. 2004b. Calibration comparisons between SEVIRI, MODIS, and GOES data. MSG RAO workshop. Salzburg, Austria

Gunshor M M, Schmit T J, Menzel W P and Tobin D. 2007. Intercalibration of the newest geostationary imagers via high spectral resolution AIRS data. Atmospheric and Environmental Remote Sensing Data Processing and Utilization III: Readiness for GEOSS, San Diego, CA. Proc. SPIE Int. Soc. Opt. Eng. 6684, 66841H

Heidinger A K, Cao C and Sullivan J T. 2002. Using moderate resolution imaging spectrometer (MODIS) to calibrate advanced very high resolution radiometer reflectance channels. *Journal of Geophysical Research*, 107 (D23): 4702

Liu J J and Li Z. 2004. A new method for cross-calibration of two satellite sensors. *International Journal of Remote Sensing*, **25**(23): 5267—5281

McMillin L M. 1975. Estimation of sea surface temperature from two infrared window measurements with different absorption. *Journal of Geographical Research*, **80**: 5113—5117

Sobrino J A and Romaguera M. 2004. Land surfacemperature retrieval from MSG1-SEVIRI data. *Remote Sensing of Environment*, **92**: 247—254

Teillet P M, Barker J L, Markham B L, Irish R R, Fedosejevs G and Storey J C. 2001. Radiometric cross-calibration of the Landsat-7 ETM+ and Landsat-5 TM sensors based on tandem data sets. *Remote Sensing of Environment*, **78**: 39—54

Vermote E F and Saleous N Z. 2006. Calibration of NOAA16 AVHRR over a dersert site using MODIS data. *Remote Sensing of Environment*, **105**: 214—220

Wan Z and Dozier J. 1996. A generalized split-window algorithm for retrieving land-surface temperature from space. *IEEE Transections on Geoscience and Remote Sensing*, **34**(4): 892—905